A High-Efficiency Dual-Frequency Rectenna for 2.45- and 5.8-GHz Wireless Power Transmission

Young-Ho Suh, *Student Member, IEEE*, and Kai Chang, *Fellow, IEEE*

***Abstract*—A dual-frequency printed dipole rectenna has been developed for the wireless power transmission at 2.45- and 5.8-GHz (industrial–scientific–medical bands). For operating at dual band, a new uniplanar printed dipole antenna is developed using a coupling method. A GaAs Schottky barrier diode analysis is performed, and a proper device requirement is discussed to have high RF-to-dc conversion efficiencies at both frequencies. A novel coplanar stripline (CPS) low-pass filter integrated with two additional open-ended T-strip CPS bandstop filters effectively block higher order harmonics generated from the diode. The measured conversion efficiencies achieved at free space are 84.4 and 82.7% at 2.45 and 5.8 GHz, respectively.**

***Index Terms*—Coplanar stripline filter, CPS low-pass filter, dual-frequency rectenna, microwave power transmission, rectenna, wireless power transmission.**

I. Introduction

THE rectenna is an important element for the wireless power transmission. Applications of the rectenna are mainly for receiving power where the physical connections are not possible. Various kinds of rectennas have been developed since Brown demonstrated the dipole rectenna using aluminum bars to construct the dipole and the transmission line [1]. He also presented the thin-film printed-circuit dipole rectenna [2] with 85% of conversion efficiency at 2.45 GHz. Linearly polarized printed dipole rectennas were developed at 35 GHz in [3] and [4] with the conversion efficiency of 39% and 70%, respectively. 5.8-GHz printed dipole rectenna was developed in 1998 [5] with a high conversion efficiency of 82%. Microstrip patch dual polarized rectennas were also developed at 2.45 GHz [6] and 8.51 GHz [7]. Recently, a circularly polarized rectenna, which does not require strict alignment between transmitting and receiving antennas, was developed at 5.8 GHz [8] with the conversion efficiency of 60%.

Several operating frequencies of the rectenna have been considered and investigated. Components of microwave power transmission have traditionally been focused on 2.45 GHz and recently moving up to 5.8 GHz, which has a smaller antenna aperture area than that of 2.45 GHz. Both frequencies have comparably low atmospheric loss, cheap components availability, and reported high conversion efficiency.

This paper presents a new dual-frequency rectenna operating at both 2.45 and 5.8 GHz (industrial–scientific–medical (ISM) bands) simultaneously. If the rectenna operates at dual band, it can be used for power transmission at either frequency depending upon power availability. A rectifying diode is analyzed to obtain design parameters for having high efficiencies at both frequencies. A diode parameter, having high conversion efficiency and insensitive to the operating frequency, is discussed. To prevent the higher order harmonics re-radiation generated by the diode, a novel coplanar stripline (CPS) low-pass filter integrated with two additional open-ended T-strip CPS bandstop filters is designed.

Manuscript received June 25, 2001.

The authors are with the Department of Electrical Engineering, Texas A&M University, College Station, TX 77843-3128 USA (e-mail: ysuh@ee.tamu.edu; chang@ee.tamu.edu).

Publisher Item Identifier 10.1109/TMTT.2002.800430.

II. Antenna and Filters Design

The structure of rectenna is illustrated in Fig. 1. The rectenna consists of a receiving dual-frequency dipole antenna, a CPS input low-pass filter, two CPS bandstop filters, a rectifying diode and a microwave block capacitor. The antenna receives the transmitted microwave power, and the input low-pass and the bandstop filters pass 2.45 and 5.8 GHz, but block the higher order harmonics from re-radiation. All microwave signals produced by the nonlinear rectifying diode, including fundamental and harmonics, are confined between the input filters and microwave block capacitor. Consequently, the conversion efficiency is improved.

All the circuit simulations including dipole antenna, CPS low-pass filter and open-ended T-strip CPS bandstop filters are designed using IE3D software [9]. IE3D utilizes full-wave electromagnetic simulation using the moment method. A low dielectric-constant substrate is suitable for designing CPS circuits to have a low attenuation. A 20-mil RT/Duroid 5870 substrate with a dielectric-constant 2.33 is used for the dual-frequency rectenna design.

A. Dual-Frequency Antenna Design

The CPS dipole dual-frequency antenna with a reflector plate is designed for 2.45 and 5.8 GHz. This type of dual-frequency antenna was introduced in [10]. In [10], the antenna radiates bidirectionally and has a double-sided structure with a microstrip feed operating at 2.4 and 5.2 GHz.

The new rectenna has a uniplanar structure, which has the advantage of convenient device mounting. A reflector plate is required for the unidirectional radiation/reception and it also increases antenna gain.

As shown in Fig. 1, a long dipole is designed for 2.45 GHz, and a short dipole is designed for 5.8 GHz. The long dipole has a length of 126.7 mm or 1.072 λ_0 at 2.45 GHz and the short dipole has a length of 45.04 mm or 0.812 λ_0 at 5.8 GHz. The feeding point has been moved about 0.8 mm from the edge of the short dipole for impedance matching. The coupling length and gap

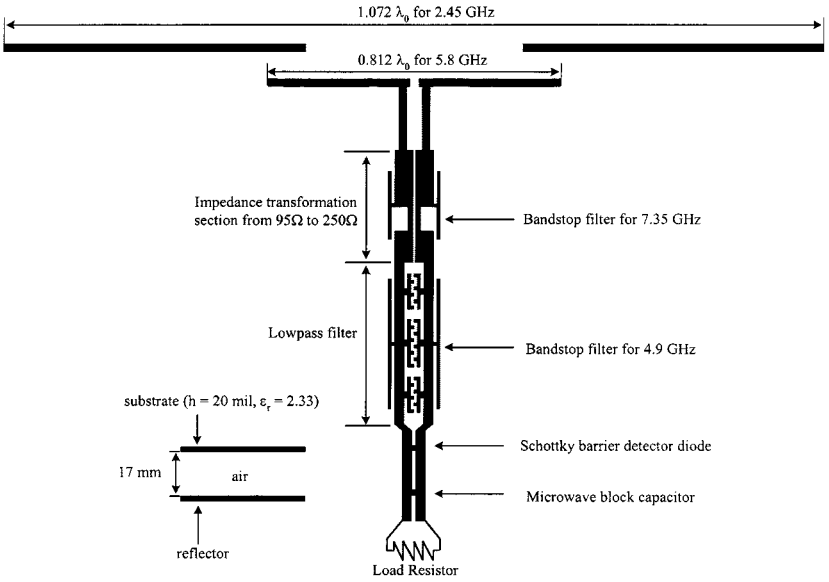

Fig. 1. Circuit configuration of the dual-frequency rectenna. The circuit is separated from a reflector plate at a distance of 17 mm.

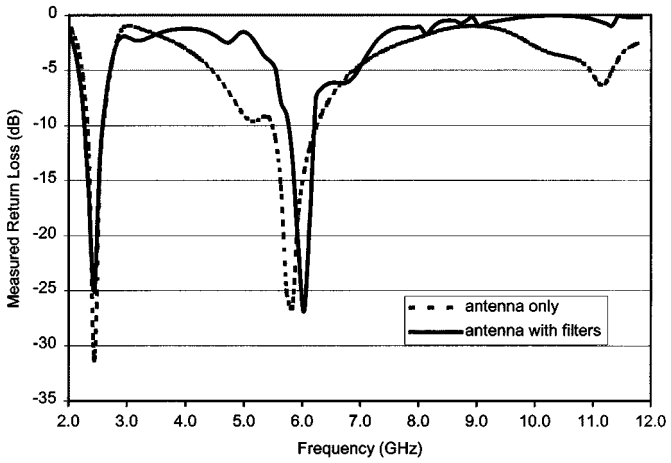

Fig. 2. Measured frequency responses of the antenna and the antenna with filters. Good return loss is achieved at both 2.45 and 5.8 GHz.

between the long and short dipole are around 6.32 and 4.2 mm, respectively. For dual-band operation, the reflector plate's distance is optimized with IE3D in order to produce good radiation patterns and similar gains for both frequencies. The reflector plate's distance is optimized at 17 mm, which is about 0.14 λ_0 of 2.45 GHz and 0.32 λ_0 of 5.8 GHz.

Measured frequency response of the antenna is shown in Fig. 2. This measurement was performed using the wide-band CPS-to-microstrip transition reported in [11], which has a less than 3-dB insertion loss and better than 10-dB return loss from 1.3 to 13.3 GHz. Measured return losses for antenna only are better than 30 and 25 dB at 2.45 and 5.8 GHz, respectively. Return losses at second order harmonics are found to be around 8.6 and 3 dB at 4.9 and 11.6 GHz, respectively.

B. CPS Low-Pass Filter Integrated With Bandstop Filters

A lumped-element CPS low-pass filter was designed in 1998 [12], and a CPS low-pass filter using a transverse slit and a parallel-coupled gap of CPS discontinuities was presented in 1999 [13]. CPS discontinuities and their applications to bandstop filters were studied by using the spur-strip and the spur-slot resonators [14]. However, structure of the reported low-pass filters are complex and design methods are not clear.

New simple CPS low-pass filter and bandstop filters are designed and shown in Fig. 3. For the low-pass filter, the capacitances take place at interdigital fingers and the CPS transmission lines work as the inductors. With this structure, the low-pass filter can be easily designed using the prototype of the desired filter type with the chosen cutoff frequency. Values of the interdigital capacitors and inductors at the desired frequency can be easily found by using IE3D [9]. The low-pass filter has a cutoff frequency of 7 GHz to pass 2.45 and 5.8 GHz and to reject 11.6 GHz, which is second order harmonic of 5.8 GHz. However, the low-pass filter will pass the second order harmonic of 2.45 GHz at 4.9 GHz and the third order harmonic level at 7.35 GHz will not be deeply suppressed.

New open-ended T-strip CPS bandstop filters, placed outside of the CPS strips, are developed for rejecting second and third order harmonics of 2.45 GHz at 4.9 and 7.35 GHz, respectively. The lengths of bandstop filters are 20.1 ($0.45\lambda_g$) and 10.5 ($0.35\lambda_g$) mm at 4.9 and 7.35 GHz, respectively.

The low-pass filter integrated with two additional open-ended T-strip bandstop filters needs to transform the antenna's input impedance of 95 Ω to the CPS characteristic impedance of 250 Ω as well as blocking higher order harmonics. An impedance transformation section consisting of two CPS step discontinuities as shown in Fig. 3, is designed and optimized by IE3D [9].

The strip width (W) and the separation gap (s) of CPS, where the rectifying diode is placed, are designed as 1.5 and 0.6 mm, respectively, which corresponds to the 184 Ω of CPS characteristic impedance (Z_0). The CPS characteristic impedance of 184 Ω is chosen to have high conversion efficiency according to the diode analysis, which will be discussed later. To accommodate interdigital capacitors for the low-pass filters, the CPS separation gap (s) is changed from 0.6 to 2.5 mm, which corre-

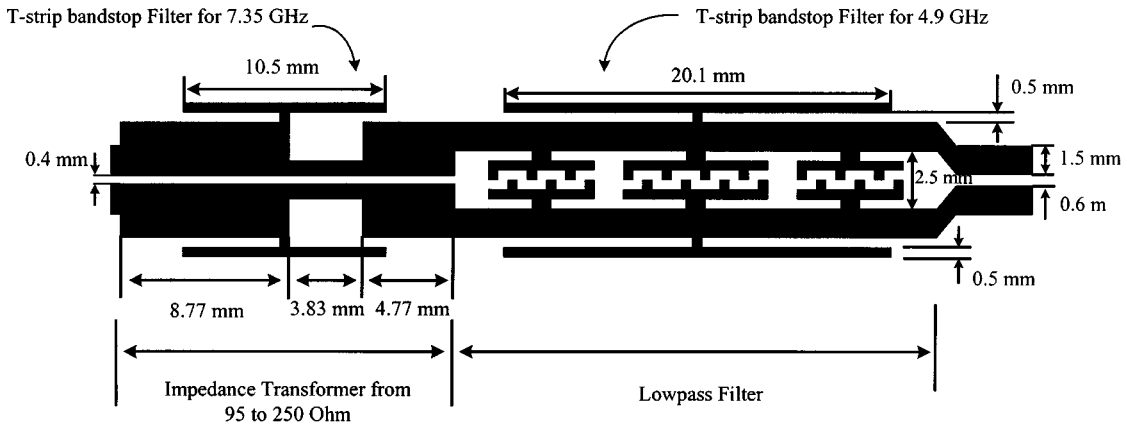

Fig. 3. The structure of CPS low-pass filter with bandstop filters.

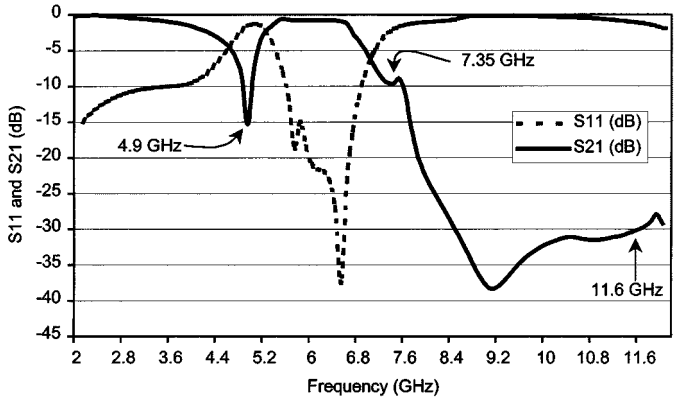

Fig. 4. Measured frequency responses of the CPS low-pass filter with bandstop filters. Low insertion losses of 0.15 and 0.75 dB are achieved at 2.45 and 5.8 GHz, respectively. Good band rejection performances were achieved at the second harmonics (4.9 and 11.6 GHz) of 2.45 and 5.8 GHz, and at the third harmonic (7.35 GHz) of 2.45 GHz.

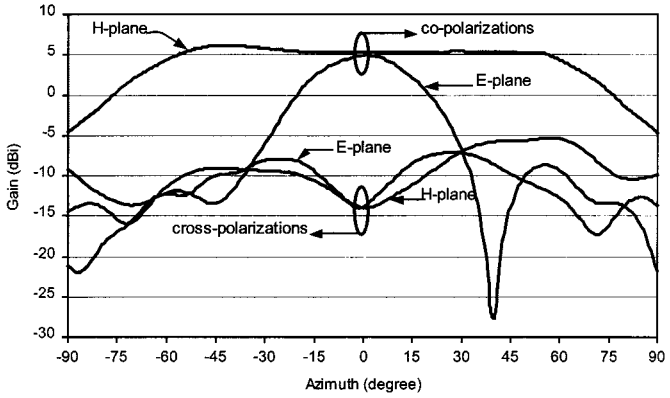

Fig. 5. Radiation patterns of the dual-frequency antenna at 2.45 GHz. E- and H-plane have similar gains and cross-polarizations are more than 18 dB for both E- and H-plane.

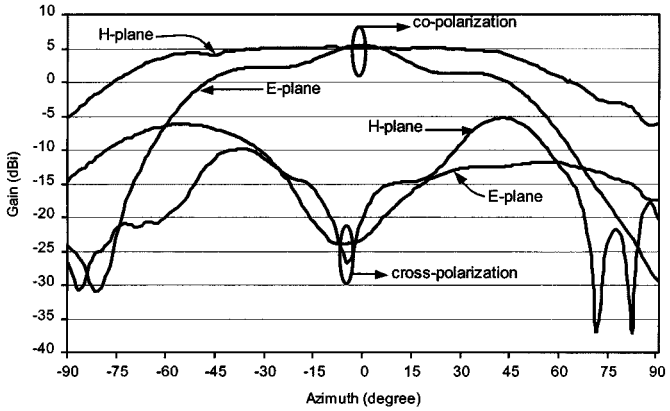

Fig. 6. Radiation patterns of the dual-frequency antenna at 5.8 GHz. E- and H-plane have similar gains and cross-polarizations are more than 25 dB for both E- and H-plane.

sponds to the impedance value changed from 184 to 250 Ω. In spite of this impedance change, little insertion loss deterioration occurs and the return loss response is better than 10 dB.

Measured frequency responses of the low-pass filter integrated with bandstop filters are shown in Fig. 4. The measurement was performed using the wide-band CPS-to-microstrip transition reported in [11]. The low insertion losses of 0.15 and 0.75 dB are achieved at 2.45 and 5.8 GHz, respectively. Band rejections at the second (4.9 GHz) and the third (7.35 GHz) harmonics of 2.45 GHz are around 15 and 10 dB, respectively, and the band rejection at the second harmonic of 5.8 GHz or 11.6 GHz is about 30 dB, which shows good bandstop performance for these harmonics.

C. Dual-Frequency Antenna Integrated With Filters

For comparison, frequency response of the antenna integrated with filters is also shown in Fig. 2. Measured return losses of 15.1 and 18.2 dB are achieved at 2.45 and 5.8 GHz, respectively. Measured return losses at the second harmonics of 2.45 and 5.8 GHz are found to be 1.58 and 0.2 dB at 4.9 and 11.6 GHz, respectively. This shows that the low-pass filter integrated with two additional bandstop filters effectively block the second order harmonics at both frequencies.

Radiation patterns of the antenna with filters are measured in the anechoic chamber. Measured radiation patterns at 2.45 and 5.8 GHz are shown in Figs. 5 and 6, respectively. Measured E-plane gains are 5 and 5.4 dBi with the 3-dB beam width of 31.5°and 36°at 2.45 and 5.8 GHz, respectively. At broadside, the cross polarization at 2.45 GHz is about 19.4 and 18.2 dB below the copolarization in E- and H-plane, respectively. At 5.8 GHz, the cross polarization is about 30.1 and 25 dB below

the co-polarization in E- and H-plane, respectively. Relatively similar E-plane gains are achieved at both 2.45 and 5.8 GHz. The measured second order harmonic radiations at both frequencies are below -10 dB for all azimuth angles.

III. Diode Analysis

A diode analysis is used to achieve high RF-to-dc conversion efficiencies at both frequencies. RF-to-dc conversion efficiency (η_d) and input impedance (Z_d) of the diode can be calculated from the closed form equations in [5], which are expressed as

$$\eta_d = \frac{1}{1+A+B+C} \tag{1}$$

where

$$A = \frac{R_L}{\pi R_s}\left(1+\frac{V_{bi}}{V_0}\right)^2 \cdot \left[\theta_{on}\left(1+\frac{1}{2\cos^2\theta_{on}}\right)-\frac{3}{2}\tan\theta_{on}\right] \tag{2}$$

$$B = \frac{R_s R_L C_j^2 \omega^2}{2\pi}\left(1+\frac{V_{bi}}{V_0}\right)\left(\frac{\pi-\theta_{on}}{\cos^2\theta_{on}}+\tan\theta_{on}\right) \tag{3}$$

$$C = \frac{R_L}{\pi R_s}\left(1+\frac{V_{bi}}{V_0}\right)\frac{V_{bi}}{V_0}(\tan\theta_{on}-\theta_{on}). \tag{4}$$

Diode input resistance is expressed as

$$R_d = \frac{\pi R_s}{\cos\theta_{on}\frac{\theta_{on}}{\cos\theta_{on}}-\sin\theta_{on}}. \tag{5}$$

R_L and R_s represent the load resistance and the series resistance of the diode, respectively. V_0 is an output voltage produced at the load resistance and V_{bi} is a diode's built-in voltage. θ_{on} is the diode conduction time in terms of radian and C_j is a junction capacitance. Closed form expression for θ_{on} and C_j are well described in [3], [5]. $\theta_{\rm on}$ is a dynamic variable dependent on input power of the diode and is determined by

$$\tan\theta_{\rm on}-\theta_{on} = \frac{\pi R_s}{R_L\left(1+\frac{V_{bi}}{V_0}\right)}. \tag{6}$$

With the known parameters, R_L, R_s, V_0 and $V_{\rm bi}$ in (6), $\theta_{\rm on}$ can be obtained. Equations (1)–(6) assumes that harmonic impedances presented to the diode by the filter network are either zero or infinity to avoid power loss by the harmonics.

RF-to-dc conversion efficiency is frequency dependent as shown in parameter B in (3). To minimize the conversion efficiency dependency to the frequency, it is necessary to minimize the effect of parameter B. Since parameter B is proportional to the square of ωC_j, a small value of C_j will reduce the effect of parameter B on the conversion efficiency. To have a small value of C_j, packaged diode is not suitable.

From the above analysis, a flip-chip type GaAs Schottky barrier diode (MA4E1317) is selected as a rectifying device. The diode has a built-in voltage ($V_{\rm bi}$) and breakdown voltage ($V_{\rm br}$) of 0.7 and 12 V, respectively. The zero bias junction capacitance (C_{j0}) is 0.02 pF with a series resistance (R_s) of 4 Ω.

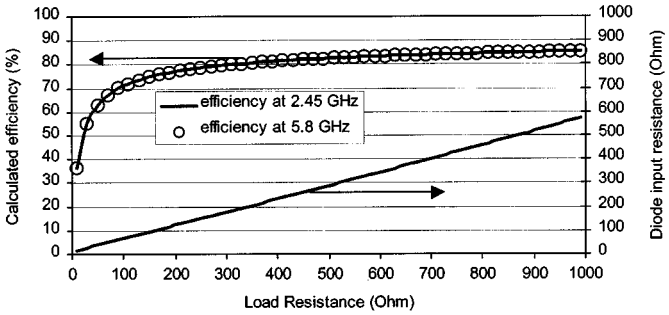

Fig. 7. Diode (MA4E1317) RF-to-dc conversion efficiency analyses in terms of the load resistance (R_L) and the diode input resistance (R_d) at 2.45 and 5.8 GHz. Diode parameter values of $V_{\rm bi}$, V_0, and $V_{\rm br}$ are 0.7, 6, and 12 V, respectively. The zero bias junction capacitance (C_{j0}) of 0.02 pF, and a series resistance (R_s) of 4 Ω are used for the analyses.

Using (1)–(6), RF-to-dc conversion efficiency (η_d) and input resistance of the diode (R_d) can be calculated in terms of load resistance (R_L) at 2.45 and 5.8 GHz, as shown in Fig. 7. In Fig. 7, very little difference in conversion efficiency is observed between 2.45 and 5.8 GHz. This is due to the low zero bias junction capacitance (C_{j0}) of the diode. Since C_{j0} is low, corresponding C_j is also low [5], and the value of parameter B is very small compared to those of parameters A and C. Consequently, parameter B, which is frequency dependent parameter, does not give much effect to the diode's conversion efficiency. From Fig. 7, the diode input resistance (R_d) and the load resistance (R_L) can be determined as design parameters for a desired target RF-to-dc conversion efficiency (η_d).

Due to the diode dimension, CPS strip width (s) is fixed to 0.6 mm and corresponding characteristic impedance is 184 Ω. The diode input impedance is matched to this impedance of 184 Ω, which corresponds to a load resistance of 310 Ω as determined in Fig. 7. This gives around 82% target efficiency. To prevent the diode breakdown due to overload, determining the limit of output dc power is necessary. Typically, the dc power level limit is determined by $P_{\rm dc} < (V_{\rm br}^2/4R_L)$ [5], where $V_{\rm br}$ is the break down voltage of the diode and R_L is the load resistance. Therefore, proper load resistance (R_L) is required as well as the proper input resistance of the diode (R_d) to have a high-efficiency and a high-output dc power.

IV. Rectenna Measurements

The rectenna is measured in free space. The measurement setup is shown in Fig. 8. Two types of power amplifiers, L0203-42 and L0505-38 (Microwave Power Inc.), are used, which can produce up to +42 and +38 dBm at 2.45 and 5.8 GHz, respectively. Standard gain horn antennas are used for transmitting power at 2.45 and 5.8 GHz, respectively. From the diode analysis described in Section III, the load resistance (R_L) is taken as 310 Ω, for 82% target efficiency.

Conversion efficiency of the rectenna is represented as

$$\eta = \frac{P_{\rm DC}}{P_{\rm received}} \times 100(\%) \tag{7}$$

where $P_{\rm DC}$ is dc power produced at the load resistance (R_L) of the rectenna and $P_{\rm received}$ is power received at antenna of

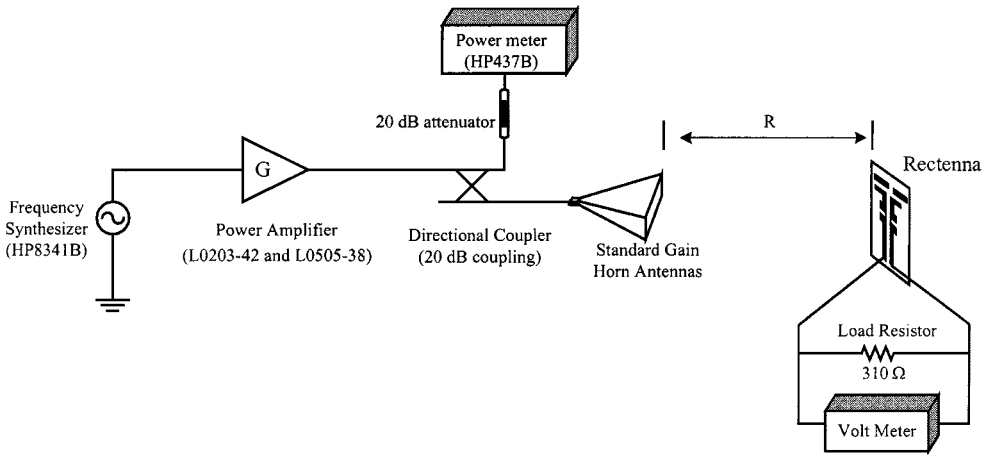

Fig. 8. Rectenna measurement setup. Two different types of power amplifiers (L0203-42 and L0505-38) and transmitting horn antennas are used for dual-frequency power transmissions.

TABLE I
RECEIVED POWER CALCULATION PARAMETERS FOR THE DUAL-FREQUENCY RECTENNA

Frequency	λ_0 (cm)	Far field (cm)	G_r (dBi)	G_t (dBi)	A_e (cm^2)
2.45 GHz	12.2	87.1	5	14.5	37.7
5.8 GHz	5.1	48.5	5.4	17.6	7.4

the rectenna. P_{received} is calculated from the Friis transmission equation expressed as

$$P_{\text{received}} = P_t \left(\frac{\lambda_0}{4\pi R}\right)^2 G_r G_t = P_t A_e \frac{G_t}{4\pi R^2} \tag{8}$$

where the effective area A_e is represented as

$$A_e = \frac{\lambda_0^2 G_r}{4\pi}. \tag{9}$$

P_t represents transmitted power. G_t and G_r represent gains of transmitter and receiver antenna, respectively. R is the distance between the transmitter and the receiver antenna. Parameters for calculating P_{received} of the dual-frequency rectenna are displayed in Table I. The efficiency is normally expressed as a function of power density. The power density is calculated by

$$P_D = \frac{P_r}{A_e} = \frac{P_t G_t}{4\pi R^2}. \tag{10}$$

Measured rectenna efficiencies are shown in Fig. 9. High efficiencies of 84.4 and 82.7% are measured at 2.45 and 5.8 GHz, respectively. Experimental efficiencies follow closely with the theoretical efficiency calculations. Received power at each highest efficiency points are 89.84 and 49.09 mW corresponding to power densities of 2.38 and 8.77 mW/cm^2 at 2.45 and 5.8 GHz, respectively, as shown in Fig. 9(b).

Measurements show that received power levels at 80% efficiency points are almost the same with 35.6 and 39.26 mW at 2.45 and 5.8 GHz, respectively. Considering the antenna's effective areas (A_e) listed in Table I, the required power density of 5.8 GHz is around 5.1 times larger than that of 2.45 GHz to achieve 80% efficiency.

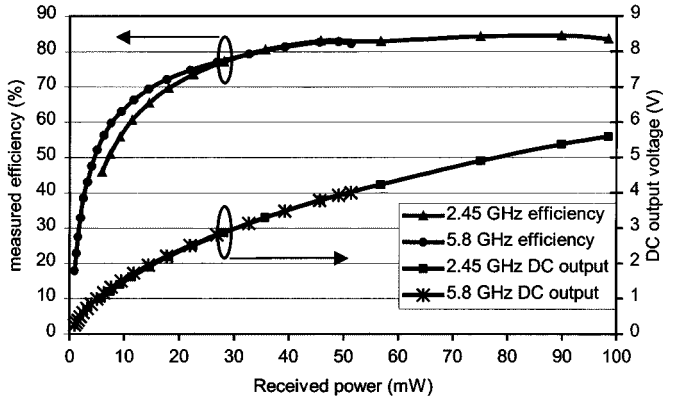

(a)

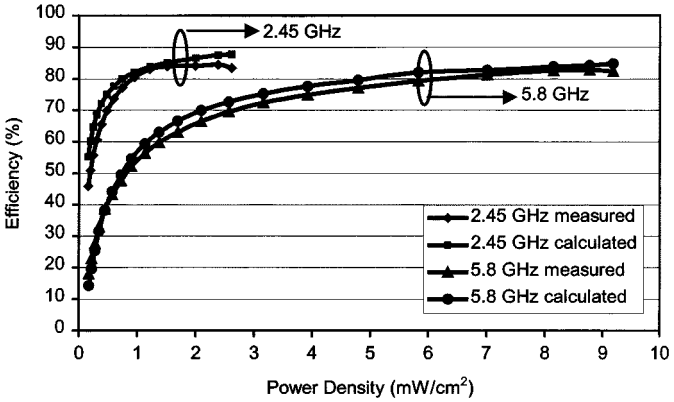

(b)

Fig. 9. RF-to-dc conversion efficiency for dual-frequency rectenna. (a) Efficiency and dc output voltage versus received power. (b) Efficiency versus power density.

According to the second order harmonic radiation measurements in Section II, the second order harmonic re-radiations at both frequencies are quite small. Observing the return loss plot of the antenna integrated with filters in Fig. 2, higher order harmonic re-radiations are expected to be small.

V. Conclusions

A dual-frequency rectenna operating simultaneously at 2.45 and 5.8 GHz has been developed. New dual-frequency printed dipole antenna is developed integrated with novel CPS filters. The antenna has E-plane gains of 5 and 5.4 dBi at 2.45 and 5.8 GHz, respectively. The combination of low-pass filter and bandstop filters effectively block the higher order harmonic re-radiations. To achieve high conversion efficiencies for the dual-frequency rectenna at both 2.45 and 5.8 GHz, diode analysis has been performed to determine the optimum diode input impedance and load resistance. A diode parameter to be considered for frequency insensitive high RF-to-dc conversion efficiency is investigated. High conversion efficiencies of 84.4 and 82.7% are achieved at 2.45 and 5.8 GHz, respectively. The dual-frequency rectenna should have many applications in wireless power transmission.

Acknowledgment

The authors would like to thank C. Wang, Texas A&M University, College Station, for technical assistance.

References

[1] W. C. Brown, "The history of power transmission by radio waves," *IEEE Trans. Microwave Theory Tech.*, vol. MTT-32, pp. 1230–1242, Sept. 1984.

[2] W. C. Brown and J. F. Triner, "Experimental thin-film, etched-circuit rectenna," in *IEEE MTT-S Int. Microwave Symp. Dig.*, 1982, pp. 185–187.

[3] T. Yoo and K. Chang, "Theoretical and experimental development of 10 and 35 GHz rectennas," *IEEE Trans. Microwave Theory Tech.*, vol. 40, pp. 1259–1266, June 1992.

[4] P. Koert and J. T. Cha, "Millimeter wave technology for space power beaming," *IEEE Trans. Microwave Theory Tech.*, vol. 40, pp. 1251–1258, June 1992.

[5] J. O. McSpadden, L. Fan, and K. Chang, "Design and experiments of a high-conversion-efficiency 5.8 GHz rectenna," *IEEE Trans. Microwave Theory Tech.*, vol. 45, pp. 2053–2060, Dec. 1998.

[6] J. O. McSpadden and K. Chang, "A dual polarized circular patch rectifying antenna at 2.45 GHz for microwave power conversion and detection," in *IEEE MTT-S Int. Microwave Symp. Dig.*, 1994, pp. 1749–1752.

[7] L. W. Epp, A. R. Khan, H. K. Smith, and R. P. Smith, "A compact dual-polarized 8.51-GHz rectenna for high-voltage (50V) actuator applications," *IEEE Trans. Microwave Theory Tech.*, vol. 48, pp. 111–120, Jan. 2000.

[8] Y. H. Suh and K. Chang, "A circularly polarized truncated-corner square patch microstrip rectenna for wireless power transmission," *Electron. Lett.*, vol. 36, no. 7, pp. 600–602, Mar. 2000.

[9] "IE3D version 8.0," Zeland Software Inc., Jan. 2001.

[10] Y. H. Suh and K. Chang, "Low cost microstrip-fed dual frequency printed dipole antenna for wireless communications," *Electron. Lett.*, vol. 36, no. 14, pp. 1177–1179, July 2000.

[11] ——, "A wideband coplanar stripline to microstrip transition," *IEEE Microwave Wireless Comp. Lett.*, vol. 11, pp. 28–29, Jan. 2001.

[12] S. G. Mao, H. K. Chiou, and C. H. Chen, "Modeling of lumped-element coplanar-stripline low-pass filter," *IEEE Microwave Guided Wave Lett.*, vol. 8, pp. 141–143, Mar. 1998.

[13] S. Uysal and J. W. P. Ng, "A compact coplanar stripline lowpass filter," in *Asia–Pacific Microwave Conf.*, vol. 2, 1999, pp. 307–310.

[14] K. Goverdhanam, R. N. Simons, and L. P. B. Katehi, "Coplanar stripline components for high-frequency applications," *IEEE Trans. Microwave Theory Tech.*, vol. 45, pp. 1725–1729, Oct. 1997.

Young-Ho Suh (S'01) received the B.S. degree in electrical and control engineering from Hong-Ik University, Seoul, Korea, in 1992, and the M.S. and Ph.D. degrees in electrical engineering from Texas A&M University, College Station, in 1998 and 2002, respectively.

From 1992 to 1996, he worked for LG-Honeywell Company Ltd., Seoul, Korea, as a Research Engineer. From 1996 to 1998, he was involved with the development of robust wireless communication systems for GSM receivers under multipath fading channels. From 1998 to 2002, he was a Research Assistant with the Electromagnetics and Microwave Laboratory, Texas A&M University. In April 2002, he joined Mimix, Houston, TX, as a Design Engineer. His research area includes uniplanar transmission line analysis and components development, microwave power transmission, antennas for wireless communications, phased array antennas and microwave integrated circuits.

Kai Chang (S'75–M'76–SM'85–F'91) received the B.S.E.E. degree from the National Taiwan University, Taipei, Taiwan, R.O.C., in 1970, the M.S. degree from the State University of New York at Stony Brook, in 1972, and Ph.D. degree from The University of Michigan at Ann Arbor, in 1976.

From 1972 to 1976, he worked for the Microwave Solid-State Circuits Group, Cooley Electronics Laboratory, The University of Michigan at Ann Abor, as a Research Assistant. From 1976 to 1978, he was with Shared Applications Inc., Ann Arbor, MI, where he was involved with computer simulation of microwave circuits and microwave tubes. From 1978 to 1981, he was with the Electron Dynamics Division, Hughes Aircraft Company, Torrance, CA, where he was involved in the research and development of millimeter-wave solid-state devices and circuits, power combiners, oscillators, and transmitters. From 1981 to 1985, he was with TRW Electronics and Defense, Redondo Beach, CA, where he was a Section Head, involved with the development of state-of-the-art millimeter-wave integrated circuits and subsystems including mixers, VCOs, transmitters, amplifiers, modulators, upconverters, switches, multipliers, receivers, and transceivers. In August 1985, he joined the Department of Electrical Engineering, Texas A&M University, College Station, as an Associate Professor, and was promoted to a Professor in 1988. In January 1990, he was appointed E-Systems Endowed Professor of Electrical Engineering. His current interests are in microwave and millimeter-wave devices and circuits, microwave integrated circuits, integrated antennas, wide-band and active antennas, phased arrays, microwave power transmission, and microwave optical interactions.

Dr. Chang has authored or coauthored *Microwave Solid-State Circuits and Applications* (New York: Wiley, 1994), *Microwave Ring Circuits and Antennas* (New York: Wiley, 1996), *Integrated Active Antennas and Spatial Power Combining* (New York: Wiley, 1996), *RF and Microwave Wireless Systems* (New York: Wiley, 2000), and *RF and Microwave Circuit and Component Design for Wireless Systems* (New York, Wiley, 2002). He also served as the editor of the four-volume *Handbook of Microwave and Optical Components*(New York: Wiley, 1989 and 1990). He is the editor of *Microwave and Optical Technology Letters* and the Wiley Book Series in *Microwave and Optical Engineering*. He has authored or coauthored over 350 technical papers and several book chapters in the areas of microwave and millimeter-wave devices, circuits, and antennas.

Dr. Chang received the Special Achievement Award from TRW in 1984, the Halliburton Professor Award in 1988, the Distinguished Teaching Award in 1989, the Distinguished Research Award in 1992, and the TEES Fellow Award in 1996 from Texas A&M University.